Measurement of Magnetic Fluctuation Induced Energy Transport

G. Fiksel, S. C. Prager, W. Shen,* and M. Stoneking
Department of Physics, University of Wisconsin, Madison, Wisconsin 53706
(Received 4 November 1993)

The local electron energy flux produced by magnetic fluctuations has been measured directly in the MST reversed field pinch (over the radial range $r/a > 0.75$). The flux, produced by electrons traveling parallel to a fluctuating magnetic field, is obtained from correlation between the fluctuations in the parallel heat flux and the radial magnetic field. The fluctuation induced flux is large (100 kW/cm^2) in the "core" ($r/a < 0.85$) and small (< 10–30 kW/cm^2) in the edge.

PACS numbers: 52.55.–s

It has long been recognized that fluctuations in the magnetic field are a potent mechanism for the anomalous transport of energy in confined plasmas. The energy transport process originates from the plasma particles' motion along the magnetic field, which can contain fluctuations in the radial direction (perpendicular to the confining equilibrium magnetic surfaces). A key feature is that the transport can be large even if the fluctuation amplitude is extremely small. If the fluctuations are resonant with the equilibrium magnetic field (i.e., the fluctuation amplitude is constant along an equilibrium field line) then a small fluctuation can introduce stochasticity to the field line trajectories. Particles following the chaotically wandering field lines can rapidly carry energy across the plasma [1,2].

After several decades of research it remains an open question whether magnetic fluctuations are responsible for anomalous transport in confinement systems, such as the tokamak, stellarator, and reversed field pinch. In all these devices, magnetic fluctuations have been measured and anomalous energy transport is observed [3]. However, causality between the two has never been proved or disproved.

In this Letter we report direct measurement of the electron energy flux specifically generated by the magnetic fluctuations in the MST reversed field pinch (RFP). The measurement was performed in the outer 25% of the minor radius ($r/a > 0.75$). We establish that magnetic fluctuation induced energy transport is large in the "core" ($r/a < 0.85$) and small in the extreme edge. To accomplish this measurement a novel diagnostic has been developed which can similarly be applied to the edge of other configurations.

Fluctuation induced transport fluxes are given by quadratic correlations of appropriate fluctuating quantities. The radial energy flux arising from electron motion parallel to the magnetic field is given by $Q_r = \mathbf{Q}_\parallel \cdot \hat{\mathbf{r}} = (\mathbf{Q}\cdot\hat{\mathbf{b}})(\hat{\mathbf{b}}\cdot\hat{\mathbf{r}})$ where $\hat{\mathbf{b}}$ and $\hat{\mathbf{r}}$ are unit vectors along the magnetic field and the radial direction, respectively. Separating $\mathbf{Q}$ and $\hat{\mathbf{b}}$ into equilibrium and fluctuating quantities yields the ensemble-averaged radial energy flux [4]

$$Q_r = \langle \tilde{Q}_\parallel \tilde{B}_r \rangle / B,$$

where $\tilde{Q}_\parallel$ is the fluctuating electron heat flux parallel to the equilibrium magnetic field [i.e., $\tilde{Q}_\parallel = \int v_\parallel (mv^2/2) \times \tilde{f}(v) dv$], $\tilde{B}_r$ is the fluctuating radial magnetic field, and B is the equilibrium field. The ensemble average $\langle\,\rangle$ is realized experimentally by averaging many time records. Since the phase of the fluctuations is random over a magnetic surface, the ensemble average approximates a magnetic surface average. A second term enters in the above expression $(\tilde{Q}_\parallel \langle \tilde{B}_\parallel \tilde{B}_r \rangle / B^2)$, but is omitted since it is measured to be small in MST. We also note that magnetic fluctuations can contribute to energy transport through the $\mathbf{E}\times\mathbf{B}$ drift that results from the fluctuating inductive electric field that accompanies the magnetic field. This mechanism is expected to be small in MST and is not considered here. Transport from fluctuating electrostatic fields has been extensively studied with Langmuir probes in the edge of many devices. The key to measuring the energy flux from fluctuating magnetic field is to obtain $\tilde{Q}_\parallel$ locally within the plasma. To this end, we have developed a fast, insertable bolometer [5].

MST [6] is a relatively large RFP ($a = 0.5$ m, $R = 1.5$ m) with moderate plasma current ($I < 0.7$ MA). To permit diagnostic insertion into the plasma, the experiments reported here were operated at reduced parameters. For measurements at the plasma edge ($r/a > 0.9$) the plasma current was maintained at 220 kA; for deeper insertion ($0.75 < r/a < 0.9$) the current was reduced to 120 kA. The line-averaged density was $(0.8\text{–}1)\times 10^{13}$ cm^{-3}, and the central electron temperature is 100–150 eV. The confinement properties and fluctuation characteristics are relatively unchanging over the full current range of MST, so that we believe that the present results are not peculiar to low current. Magnetic fluctuations have been studied extensively in MST [4,7,8]. Nearly all the fluctuation power (> 90%) resides in several modes at low frequency ($f < 30$ kHz) with poloidal and toroidal mode number $m = 1$ and $n = 5$–8. Detailed comparison between the nonlinear magnetohydrodynamics (MHD) computation and experimental measurements, including details of nonlinear coupling [9], has established that the fluctuations are nonlinearly coupled, global, tearing modes resonant in the core. These modes are capable of breaking the magnetic surfaces within the reversal surface (at $r/a \approx 0.85$). The higher frequency fluctuations ($f > 50$ kHz) are small

0031-9007/94/72(7)/1028(4)$06.00

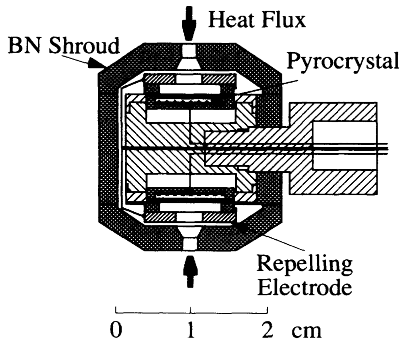

FIG. 1. Schematic of the pyrobolometer.

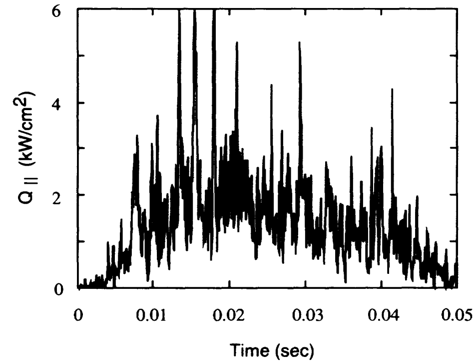

FIG. 2. Parallel heat flux $Q_\parallel$ at 4 cm from the wall ($r/a=0.92$).

scale turbulence resonant with the local magnetic field. Their origin is not yet established.

The parallel electron heat flux was measured with a fast pyrobolometer [5], capable of detecting the fluctuations, $\tilde{Q}_\parallel$. The schematic of the bolometer is shown in Fig. 1. The heart of the bolometer is a pyrocrystal of $LiNbO_3$. The diameter of the crystal is 1 cm and the thickness is 1 mm. When exposed to a plasma (or any other source of thermal energy) the crystal generates electric current that is proportional to the absorbed power. The signal is measured with a fast current-to-voltage converter. The pyrocrystal itself was absolutely calibrated and the frequency bandwidth was measured to be 150 kHz. The sensitivity of the bolometer is 1.8×10^{-8} A/W. The range of measurable fluxes is 0.1 W/cm^2–10 kW/cm^2. We did not observe any noticeable microphonic effect, in part due to the spring suspension of the crystal. Details of calibration and the design can be found in Ref. [5].

Both sides of the crystal are metalized and the side exposed to the plasma is grounded. The main source of the heat flux at the plasma edge is electrons streaming along the magnetic field lines. The electrons enter the bolometer through a small aperture (1 mm in diameter and 1 mm in length) in the protective boron nitride shroud. The bolometer is two sided; therefore, when aligned along magnetic lines it measures the field aligned heat flux simultaneously in two opposite directions, which yields the net flux.

With the biased repelling electrode we could either detect the plasma electron energy distribution function or gate the electron flux. The gating decreases the total energy deposited into the bolometer, so the bolometer can be inserted deeper into the plasma without damage. In the experiments described below the bolometer is gated with a duration of 2 ms during the plasma current flattop. The geometric transparency of the entrance aperture was evaluated by a Monte Carlo simulation of the incoming electron flux in the magnetic field, using the measured electron distribution function [10]. The calculated transparency is about 50%, in agreement with the value inferred from other bolometric measurements in MST [10].

The fluctuation of the magnetic field was measured by a miniature magnetic coil. The poloidal separation of the bolometer and the magnetic probe was 10 cm. This separation eliminates probe shadowing and interference effects. On the other hand, it is well within the parallel correlation length of ~0.5–1 m for the dominant $m=1$ tearing modes in the MST. The geometric size of both probes is 1–2 cm which is also much less than the parallel correlation length and the dominant $m=1$ wavelength (≈ 1 m). Therefore, perturbation to the plasma should be kept to a minimum. The radial separation of the two probes was kept within ±0.5 cm, which is less than the radial correlation length, measured to be about 5 cm for the dominant frequency [10].

The parallel heat flux measured by the bolometer is shown in Fig. 2, for the forward (parallel to the electron drift) direction. The equilibrium component of the heat flux has a large anisotropy, with the heat flux in the electron drift direction dominating by a factor of 5 to 10 (Fig. 3). Measurements with an electron energy analyzer (EEA) [10] reveal that in MST, as in other RFPs [11], the current at the cold edge is dominated by fast electrons which can be described as a drifted bi-Maxwellian with $T_\parallel\approx 80$–115 eV and $T_\perp\approx 20$–30 eV and $E_{\rm drift}=mv_{\rm drift}^2/2\approx 10$–20 eV. These particle flux measurements are consistent with the pyrobolometer heat flux

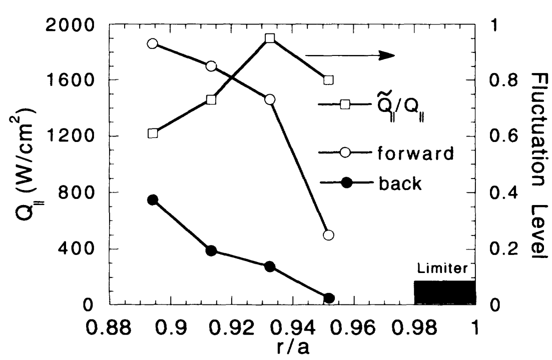

FIG. 3. Radial distribution of the parallel heat flux and its relative fluctuation amplitude. The forward direction corresponds to the direction of fast electrons drift.

measurements, if we relate the heat flux and particle flux as $Q_{\parallel} = (j_{\parallel}/e)(\frac{3}{2}T_{\parallel} + T_{\perp} + E_{\text{drift}})$. For the measured $Q_{\parallel} = 2000$ W/cm^2 we find that the fast electron current density $j_{\parallel} \approx 10$ A/cm^2, roughly 75% to 100% of the total current density. The fast electron temperature inferred from a repeller voltage scan of the pyrobolometer also agrees with EEA measurements. An additional salient feature of the parallel heat flux is the large bursts, which coincide with the crash of sawtooth oscillations.

The fluctuations in the parallel heat flux, $\tilde{Q}_{\parallel}$, are large, roughly 50%, as is evident from Fig. 2. The relative fluctuation amplitude is about 80%–100% at the plasma edge and decreases toward the plasma center, as seen in Fig. 3. The frequency spectra of $\tilde{Q}_{\parallel}$ and $\tilde{B}_r$ are similar [Fig. 4(a)], with both peaking at low frequency. The peak at the extreme low end of the bandwidth represents the sawtooth oscillations. The gentle peak apparent at about 10 kHz in both signals arises from the tearing oscillations.

To determine the radial energy flux driven by these fluctuations [Eq. (1)] we have evaluated the cross coherence between $\tilde{Q}_{\parallel}$ and $\tilde{B}_r$ from an ensemble of 60–120 reproducible discharges. The magnitude and phase of the cross coherence are displayed in Figs. 4(b) and 4(c) (for $r/a = 0.75$). The coherence is strong and restricted to low frequency (≈ 10 kHz). This coherence arises from the several dominant tearing fluctuations. The coherence decreases with radius, reaching ≈ 0.2 at $r/a = 0.85$ (reversal surface) and ≈ 0.3 at $r/a = 0.95$. The cross-power frequency spectrum is displayed in Fig. 4(d). It is clear that the energy flux from magnetic fluctuations arises mainly from the low frequency tearing oscillations. The higher frequency microturbulence has a weak cross coherence and low amplitude; hence, it does not contribute significantly to the energy flux from magnetic fluctuations. The cross phase at the frequency of maximum coherence is about 60°, not optimal for transport. However, the resulting energy flux can be large since the fluctuation amplitudes are large.

From the coherence measurements the radial energy flux, $Q_r = \langle \tilde{Q}_{\parallel} \tilde{B}_r \rangle / B$, is calculated. The radial profile of the energy transport is shown in Fig. 5. Also shown is the magnetic energy transport flux relative to the total energy flux, which is the Ohmic power normalized to the magnetic surface area at the corresponding radius. Precise determination of the radial dependence of the total energy flux requires profile information which is not available. We see that at the plasma edge the heat transport from magnetic fluctuations is low, but inside the reversal surface ($r/a < 0.85$) it constitutes a significant fraction of the total flux. The observed radial dependence of the anomalous transport is consistent with expectation of field line stochasticity. It is anticipated from MHD computation that the magnetic surfaces within the reversal surface are broken by the dominant magnetic fluctuations resonant in the core. The edge magnetic surfaces are not similarly disturbed since the tearing fluctuations are not resonant in that region.

We conclude with four points, two of which are general and two focused on the RFP. First, we have definitely, by measuring the local $\tilde{Q}_{\parallel}$ and $\tilde{B}_r$, and their correlation, demonstrated that magnetic fluctuations can drive significant energy transport. This demonstration is definitive since we have directly measured the energy flux driven by magnetic fluctuations. The radial profile and frequency dependence of the fluctuation induced flux are in accord with the expectation that internally resonant

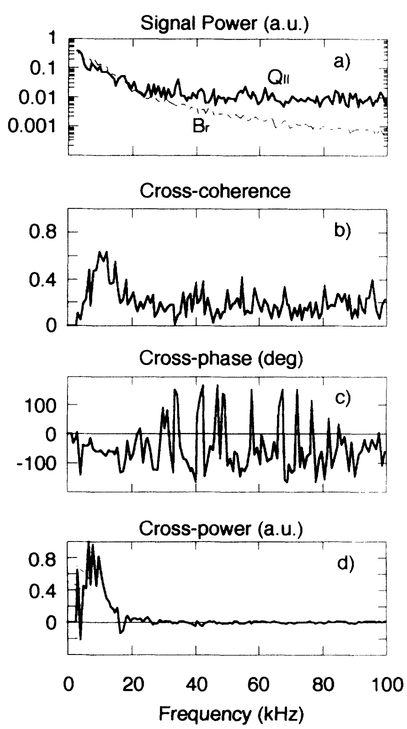

FIG. 4. Frequency spectra of (a) fluctuation of $Q_{\parallel}$ and B_r, (b) cross coherence of $Q_{\parallel}$ and B_r, (c) cross phase, and (d) cross power.

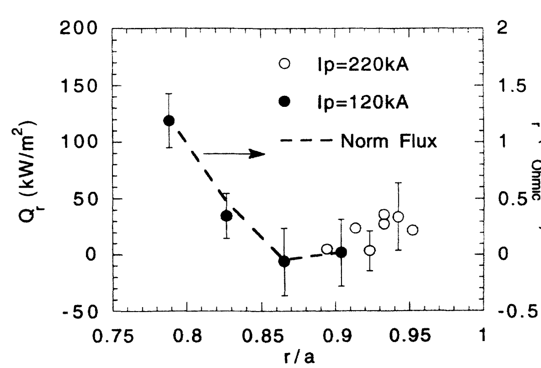

FIG. 5. Radial profile of magnetic fluctuation induced heat transport $Q_r = \langle \tilde{Q}_{\parallel} \tilde{B}_r \rangle / B$. The dashed line shows the fluctuation heat transport relative to the total energy flux, which is Ohmic power (P_{Ohmic}) normalized to the magnetic surface area at the corresponding radius.

tearing oscillations are responsible for the transport. In the extreme edge, where the tearing oscillations do not break magnetic surfaces, the energy flux from magnetic fluctuations is small. Second, the technique, based on the development of a fast, insertable bolometer, can be applied to the edge of other experiments, such as tokamaks and stellarators, to similarly discover the contribution of magnetic fluctuations to transport. Third, the cause of anomalous energy transport in the extreme edge of the RFP remains unknown. Earlier work [12–14] indicates that electrostatic fluctuations, operating on the bulk of the electron velocity distribution function, are not responsible. In MST we will be exploring the contribution of electrostatic transport of fast electrons.

Finally, with the present results, the RFP concept might be in the unique position of being accompanied by a basic understanding of the origin of both the dominant fluctuations and the anomalous energy transport. This feature is subject to the caveat that the results reported here were limited to one device under restricted conditions. Nonetheless, a physics basis now exists for the control of fluctuations and transport in the RFP, and appropriate techniques are presently being formulated.

The authors appreciate discussions with many MST group members. This work has been supported by the U.S. Department of Energy.

*Present address: Department of Electrical and Computer Engineering, University of Wisconsin, Madison, WI 53706.

[1] J. D. Callen, Phys. Rev. Lett. **39**, 1540 (1977).
[2] A. B. Rechester and M. N. Rosenbluth, Phys. Rev. Lett. **40**, 38 (1978).
[3] P. S. Lewer, Nucl. Fusion **25**, 543 (1985).
[4] S. C. Prager, Plasma Phys. Controlled Fusion **32**, 903 (1990).
[5] G. Fiksel, D. Holly, and J. Frank, Rev. Sci. Instrum. **64**, 2761 (1993).
[6] R. N. Dexter *et al.*, Fusion Technology **19**, 131 (1991).
[7] A. F. Almagri *et al.*, Phys. Fluids B **4**, 4080 (1992).
[8] J. S. Sarff *et al.*, Phys. Fluids B **5**, 2540 (1993).
[9] S. Assadi, S. C. Prager, and K. L. Sidikman, Phys. Rev. Lett. **69**, 281 (1992).
[10] M. Stoneking *et al.*, Bull. Am. Phys. Soc. **38**, 4S2 (1993).
[11] J. C. Ingraham *et al.*, Phys. Fluids B **2**, 143 (1990).
[12] H. Ji *et al.*, Phys. Rev. Lett. **67**, 62 (1991).
[13] T. D. Rempel *et al.*, Phys. Fluids B **4**, 2136 (1992).
[14] H. Y. W. Tsui, Nucl. Fusion **28**, 1543 (1998).

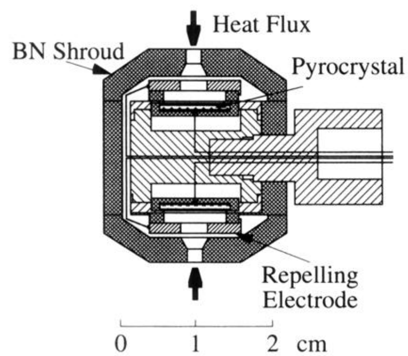

FIG. 1. Schematic of the pyrobolometer.

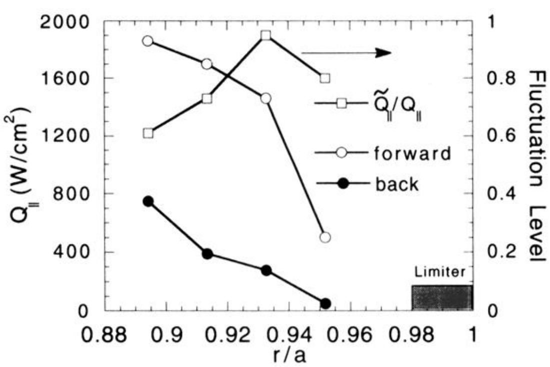

FIG. 3. Radial distribution of the parallel heat flux and its relative fluctuation amplitude. The forward direction corresponds to the direction of fast electrons drift.